The Journal of Chemical Physics

RESEARCH ARTICLE | JANUARY 18 2024

Kinetics of physical aging of a silicate glass following temperature up- and down-jumps FREE

Ricardo F. Lancelotti ; Edgar D. Zanotto ; Sabyasachi Sen

J. Chem. Phys. 160, 034504 (2024)
https://doi.org/10.1063/5.0185538

The Journal of Chemical Physics ARTICLE pubs.aip.org/aip/jcp

Kinetics of physical aging of a silicate glass following temperature up- and down-jumps

Cite as: J. Chem. Phys. 160, 034504 (2024); doi: 10.1063/5.0185538
Submitted: 31 October 2023 • Accepted: 22 December 2023 •
Published Online: 18 January 2024

Ricardo F. Lancelotti,[1,2,a)] Edgar D. Zanotto,[1] and Sabyasachi Sen[2]

AFFILIATIONS

[1] Federal University of São Carlos, Graduate Program in Materials Science and Engineering, São Carlos, São Paulo 13565-905, Brazil
[2] Department of Materials Science and Engineering, University of California at Davis, Davis, California 95616, USA

[a)] **Author to whom correspondence should be addressed:** lancelotti.r@dema.ufscar.br

ABSTRACT

In this article, we investigate the structural relaxation of lithium silicate glass during isothermal physical aging by monitoring the temporal evolution of its refractive index and enthalpy following relatively large (10–40 °C) up- and down-jumps in temperature. The Kohlrausch–Williams–Watts function aptly describes the up- and down-jump data when analyzed separately. For temperature down-jumps, the glass exhibits a typical stretched exponential kinetic behavior with the non-exponentiality parameter $\beta < 1$, whereas up-jumps show a compressed exponential behavior ($\beta > 1$). We analyzed these datasets using the non-exponential and non-linear Tool–Narayanaswamy–Moynihan (TNM) model, aiming to provide a comprehensive description of the primary or α-relaxation of the glass. This model described both up- and down-jump datasets using a single value of $\beta \leq 1$. However, the standard TNM model exhibited a progressively reduced capacity to describe the data for larger temperature jumps, which is likely a manifestation of the temperature dependence of the non-exponentiality or non-linearity of the relaxation process. We hypothesize that the compressed exponential relaxation kinetics observed for temperature up-jumps stems from a nucleation-growth-percolation-based evolution on the dynamically mobile regions within the structure, leading to a self-acceleration of the dynamics. On the other hand, temperature down-jumps result in self-retardation, as the slow-relaxing denser regions percolate in the structure to give rise to a stretched exponential behavior.

I. INTRODUCTION

When a material is cooled below its melting point and crystallization is kinetically prevented, it remains as a metastable supercooled liquid (SCL). As this SCL is further cooled toward its glass transition region, its atomic structure freezes on laboratory timescales, reaching the so-called fictive temperature T_f. At temperatures $T < T_f$, the resultant glassy state is not in thermodynamic equilibrium.[1,2] Consequently, glasses spontaneously undergo structural relaxation, a gradual adjustment of their atomic arrangement, in response to changes in the external thermodynamic variables, such as temperature or pressure. This relaxation aims to achieve a metastable equilibrium with the newly imposed conditions.[3] Given enough time at any temperature, they crystallize, reaching thermodynamic equilibrium.[4]

Understanding structural relaxation and its dependence on thermal history is key to designing new glass products or optimizing the performance of functional glasses. This is because changes in the atomic structure impact all their physical properties.[5–7] The structural relaxation phenomenon can be studied through physical aging experiments, which typically involve monitoring subtle changes in various physical properties, such as refractive index,[8–11] density,[12–15] or enthalpy,[16–19] over time, during or after changes in temperature below the glass transition temperature (at $T < T_g$). As the glass evolves from its initial to its final equilibrium state, the rate at which these properties evolve depends on the actual temperature the glass is subjected to, as well as on its T_f, which also evolves over time as a function of thermal history.[20]

When a glass undergoes isothermal aging following a temperature jump, any physical property p evolves with aging time t from its initial value p_0 to its final value p_∞ such that a normalized relaxation function

$$\phi(t) = \frac{p(t) - p_\infty}{p_0 - p_\infty}. \quad (1)$$

According to this definition, $\phi(t)$ is unity for $t = 0$, i.e., at the onset of the temperature jump, and zero for a fully relaxed system

when equilibrium is reached at the new temperature at sufficiently long times. Several models have been proposed to describe the primary or α-relaxation process in glass-forming systems. For instance, the Kohlrausch–Williams–Watts (KWW)[21,22] function describes the temporal decay of $\phi(t)$ as

$$\phi(t) = \exp\left[-\left(\frac{t}{\tau_K}\right)^{\beta}\right], \tag{2}$$

where τ_K is the characteristic relaxation time of the system and β is the non-exponentiality parameter. This function describes a stretched (compressed) exponential relaxation kinetics for $0 < \beta < 1$ ($\beta > 1$), while a purely exponential relaxation is recovered for $\beta = 1$.[23–25] These parameters are related to the average relaxation time $\langle\tau\rangle$ via the following expression: $\langle\tau\rangle = \frac{\tau_K}{\beta}\Gamma\left(\frac{1}{\beta}\right)$, where Γ is the gamma function. A combination of Eqs. (1) and (2) yields the temporal evolution of any property $p(t)$ as

$$p(t) = p_\infty + (p_0 - p_\infty)\exp\left[-\left(\frac{t}{\tau_K}\right)^{\beta}\right]. \tag{3}$$

Phillips[26,27] proposed a relaxation model based on diffusion to traps to obtain limiting values of β of either 3/5 or 3/7 near T_g. However, a large number of studies show that rather than remaining constant, β decreases with a decrease in the temperature.[7,10,28,29] Concerning the origin of the stretched exponential relaxation, two potential explanations can be presented.[30] The relaxation process can be stretched as a result of the spatial dynamical heterogeneities arising from fluctuations in density and composition within glass forming systems. This heterogeneous dynamics is characterized by locally exponential relaxation with a spatiotemporally varying time constant τ. Consequently, the relaxation of the ensemble can be expressed as a sum of exponentials, each with a different τ, giving rise to a global non-exponential decay.[30,31] This scenario is formally equivalent to a distribution of relaxation times $f(\tau)$, which relates to the relaxation function as

$$\phi(t) = \int_0^\infty f(\tau)e^{-t/\tau}d\tau. \tag{4}$$

The distribution function $f(\tau)$ is subject to the constraint: $\int_0^\infty f(\tau)d\tau = 1$. This equation can be closely approximated by a Prony series,

$$\phi(t) = \sum_{i=1}^{N} w_i \exp\left(-\frac{t}{\tau_i}\right), \tag{5}$$

where the weighting factors w_i satisfy $\sum_{i=1}^{N} w_i = 1$. In this case, the non-exponentiality parameter β is a measure of the width of this distribution $f(\tau)$, where a lower value of β corresponds to a wider distribution and vice versa.

In contrast, in a homogeneous dynamical scenario, the stretching of the relaxation originates from cooperativity in a hierarchical sequence of events. Here, the relaxation is intrinsically non-exponential, with a lower value of β signifying stronger cooperativity.[32] Finally, several studies have reported that, in some cases, the relaxation dynamics can be faster than exponential, i.e., a compressed exponential with $\beta > 1$.[24,33–41] It should be noted here that a compressed exponential function cannot be expressed as a sum of exponentials, but may originate from a sum of Gaussian decay functions,[35]

$$\phi(t) = \sum_{i=1}^{N} w_i \exp\left[-\left(\frac{t}{\tau_i}\right)^2\right]. \tag{6}$$

For instance, Diaz Vela and Simmons[39] performed simulations of model polymeric and small-molecule glass-formers in the iso-configurational ensemble and observed that non-exponential relaxation is not solely a consequence of spatial averaging over a distribution of locally exponential processes, and it cannot be interpreted as a direct measure of dynamic heterogeneity through spatial averaging. A range of non-exponential relaxation behavior is displayed even at the level of a single particle without time averaging. Their findings indicate that faster-relaxing particles in low-density regions of a liquid tend to exhibit locally stretched relaxation, while slower-relaxing particles in high-density regions show compressed relaxation. Jaeger and Simmons,[41] in their physical aging experiments involving up- and down-jumps in temperature, identified compressed exponential relaxation in up-jump experiments with large temperature jumps. It should be noted that up-jump aging experiments are characterized by a reduction in glass density as T_f increases over time.[12,13] In separate experiments conducted by Guerette *et al.*,[37] a silica glass was densified under hot compression at 4 GPa and 1100 °C (T_g of ~1200 °C). This led to a significant increase in the refractive index, from 1.461 to 1.525, and in density, from 2.20 to 2.53 g/cm^3. Then, the glass structure was isothermally relaxed at 850 °C. During this process, the refractive index returned to its initial value of ~1.461 and the density to 2.20 g/cm^3, a behavior similar to that observed in temperature up-jump experiments. In this case, relaxation followed a compressed exponential decay of index and density with $\beta = 1.28$.

A down-jump in fictive temperature is the predominant method employed to investigate physical aging. In this approach, the melt-quenched glass can be readily aged at a temperature below T_g, resulting in an increase in density. In contrast, conducting an up-jump experiment to decrease the density involves the time-consuming initial step of lowering T_f for several days or even weeks before initiating the actual up-jump procedure.

The shape of the relaxation function in up- and down-jump experiments is, however, expected to be distinctly different. The down-jump data typically display a stretched exponential relaxation, while many of the up-jump data exhibit a compressed exponential recovery.[12,13,42,43] This difference in kinetics between the up- and down-jump experiments is a manifestation of the fact that the relaxation rate in the glassy state not only depends on the actual temperature but also on the fictive temperature T_f of the glass, where the latter evolves over time differently for the two experiments. In other words, this difference in kinetics results from the non-linear effect of the intrinsic structural changes during physical aging that has been described traditionally in the glass literature by the Tool–Narayanaswamy–Moynihan (TNM) model.[3,20,44] In this model, t/τ is replaced by the reduced time ξ, resulting in the restoration of linearity,[3,45]

$$\xi(t) = \int_0^t \frac{dt'}{\tau(t')}. \tag{7}$$

To distinguish the up-jump experiment from the down-jump experiment, one can employ a relaxation function δ instead of using the normalized relaxation function [Eq. (1)]. This function represents a fractional departure of an instantaneous property value $p(t)$ from the equilibrium value p_∞,

$$\delta(t) = \frac{p(t) - p_\infty}{p_\infty}. \tag{8}$$

It is easy to see that $\phi(t) = \frac{\delta(t)}{\delta_0}$, where δ_0 is the initial value of the relaxation function ($\delta_0 = \frac{p_0 - p_\infty}{p_\infty}$). Thus, a glass equilibrated at a temperature T_0 and then exposed to a temperature T will change its fictive temperature T_f over time according to[42]

$$\frac{\delta(t)}{\delta_0} = \frac{T_f(t) - T}{T_0 - T}. \tag{9}$$

Moreover, the relaxation function introducing the reduced time is given by

$$\frac{\delta(t)}{\delta_0} = \exp\left[-\left(\int_0^t \frac{dt'}{\tau(t')}\right)^\beta\right]. \tag{10}$$

Combining Eqs. (9) and (10), in the TNM model, T_f can be expressed as

$$T_f(t) = T + (T_0 - T)\exp\left[-\left(\int_0^t \frac{dt'}{\tau(t')}\right)^\beta\right], \tag{11}$$

where the relaxation time τ incorporates a non-linearity parameter $0 \le x \le 1$ to consider the contributions of both T and T_f,[20]

$$\tau = A\exp\left(\frac{x\Delta h^*}{RT} + \frac{(1-x)\Delta h^*}{RT_f}\right), \tag{12}$$

where A is the pre-exponential constant, R is the universal gas constant, and Δh^* is the activation energy for the relaxation process.

While the TNM model is widely utilized in the literature, its phenomenological nature does not provide a clear insight into the physical origin of the non-linearity parameter x, its temperature dependence, or whether it should be related to the non-exponentiality parameter β. Moreover, the inadequacy of the TNM model for large temperature jumps (larger than 30 °C in a silicate glass, which corresponds to a magnitude of ~4.2% in terms of $\Delta T/T_g$) was highlighted by Moynihan himself during a discussion session,[46] as well as by other authors under similar circumstances.[47–50] Therefore, in this study, we have conducted a series of physical aging experiments to systematically test the validity of the TNM model monitoring two different properties (enthalpy and refractive index) following large temperature jumps (up to 40 °C below T_g ($\Delta T/T_g$ = 5.5%). The lithium disilicate glass ($Li_2Si_2O_5$, LS_2) was chosen to investigate the structural relaxation because of its excellent thermal stability against moisture and crystallization for long physical aging experiments below T_g.

II. EXPERIMENTAL DETAILS

A. Sample preparation

The LS_2 glass was synthesized using the conventional melt-quenching method, wherein stoichiometric mixtures of SiO_2 and Li_2CO_3 were melted in a platinum crucible at 1400 °C for 1 h. The melt was poured onto a steel slab and pressed under a steel plate. To improve the chemical homogeneity, the glass was quenched and re-melted three times. Subsequently, the glass was annealed at 390 °C for 2 h, followed by slow cooling to room temperature, allowing for the subsequent step of cutting the samples. The LS_2 glass used in this study is from the same batch used in previous works,[10,11,51] with T_g of 454 °C as measured by differential scanning calorimetry (DSC).

For the refractive index measurements, two samples (referred to here as sample I and sample II) of ~10 × 10 × 3 mm^3 were cut using a diamond saw, and their two perpendicular faces were polished to optical quality. Initially, the starting fictive temperature T_0 of samples I and II was set by annealing the samples at 447 °C for 4 h (a few degrees below T_g).

For the enthalpy measurements, we initiated by annealing a sample of similar dimensions (10 × 10 × 3 mm^3) at a temperature 40 °C below its T_g for 15 days (414 °C, starting temperature T_0), aiming to lower T_f. We annealed the sample at 414 °C (40 °C below T_g) for 15 days based on the results of a previous study on refractive index relaxation, which indicated that, at 412 °C, the same LS_2 glass required 7 days to relax by 99% and 14 days to achieve practical equilibrium (99.9% relaxed).[11] This sample was then fragmented into multiple small pieces for the subsequent aging experiments and enthalpy measurements. Some of these pieces were heat-treated at another starting temperature, 454 °C for 6.5 h.

B. Refractive index and enthalpy relaxation measurements

Structural relaxation during physical aging experiments was followed by monitoring changes in refractive index and enthalpy. We performed up- and down-jump experiments in which the samples were first equilibrated at T_0 for a specified initial time t, as shown in Table I. Next, the samples were aged at temperature T until a constant value within the experimental error was reached. Some refractive index relaxation data were collected and reported in our previous study.[11]

The refractive index relaxation experiments using sample I were performed for jumps ending at the same temperature of

TABLE I. Parameters used in each physical aging experiment.

	t in T_0	T_0 (°C)	T (°C)	References
Ref. index, sample I	4 h	447	432	11
Ref. index, sample I	32 days	412	432	...
Ref. index, sample II	4 h	447	422	11
Ref. index, sample II	20 days	422	447	...
Enthalpy	15 days	414	444	...
Enthalpy	15 days	414	454	...
Enthalpy	6.5 h	454	444	...

432 °C. A temperature down-jump was executed from 447 to 432 °C, and the refractive index was monitored over time, as reported in a previous study.[11] Subsequently, the same sample was rejuvenated by being annealed again at 447 °C for 4 h, followed by equilibrating at 412 °C for ~32 days. In the present work, we utilized this sample equilibrated at 412 °C to conduct an up-jump experiment at 432 °C. For sample II, we conducted the down-jump from 447 to 422 °C, which lasted ~20 days, and subsequently, we performed the up-jump to 447 °C.

All refractive index measurements were carried out at room temperature after quenching the samples following each annealing treatment. More specifically, the evolution of the refractive index during aging was followed by periodically taking the sample out of the furnace at the end of each time step, quenching it in air and stabilizing it for 20 min, performing an index measurement, and inserting it back into the furnace for the next time step (i.e., the heat treatment was accumulative) until a constant index value was reached. The refractive index was measured at a wavelength λ of 546.1 nm (e-line) using a high-precision V-block Carl Zeiss Jena Pulfrich-refractometer PR2, equipped with a VoF5 glass prism ($n_{\lambda,p}$ = 1.748 005 at the e-line). The reported refractive index values are an average of 10 consecutive measurements, which enabled the determination of the standard deviation. The refractometer measures the angle of the refracted beam γ from a sample positioned on the V-prism with a thin layer of immersion oil. The wavelength-dependent refractive index n_λ is correlated with the VoF5 prism through the following equation:

$$n_\lambda = \sqrt{n_{\lambda,p}^2 - \cos(\gamma)\sqrt{n_{\lambda,p}^2 - \cos^2(\gamma)}}. \tag{13}$$

The enthalpy relaxation measurements were performed by annealing each small piece for a certain time period at a specific temperature T in a Mettler Toledo DSC1 under nitrogen atmosphere. For each experimental run, (10 ± 1) mg of the sample pre-equilibrated at 414 or 454 °C was inserted into hermetically sealed aluminum pans. The isothermal temperature jump experiments comprised a series of steps. The initial step was aging the sample at a temperature T for a certain time, as schematized in Fig. 1, exemplifying an aging experiment at 444 °C for 60 min. Once the target aging temperature was reached on the DSC equipment, the sample was inserted to initiate the experiment. After the aging period, which ranged from 5 min up to 4 h, the sample was cooled from the aging temperature to 300 °C (T_a) at a rate of 100 °C/min. This cooling step was followed by a 5 min holding period at 300 °C to ensure thermal stabilization. Subsequently, the sample was heated to 515 °C (T_b) at a rate of 10 °C/min, resulting in the DSC scan for the aged sample. Following this scan, the sample was cooled from 515 to 300 °C at 10 °C/min and held at 300 °C for 5 min, followed by a heating scan at 10 °C/min to generate the rejuvenated sample. The enthalpy recovery ΔH_R as a function of aging time at a given aging temperature was determined by subtracting the rejuvenated DSC heat flow curve ($\dot{Q}_{rejuv}$) from the aged DSC heat flow curve ($\dot{Q}_{aged}$) and integrating as follows:

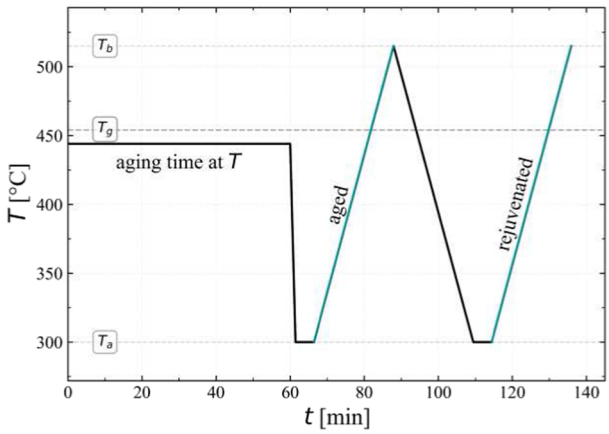

FIG. 1. Schematic diagram of the physical aging protocol for enthalpy recovery experiments, illustrating an aging experiment at 444 °C for 60 min.

$$\Delta H_R = \frac{1}{q_h}\int_{T_a}^{T_b}\left(\dot{Q}_{aged} - \dot{Q}_{rejuv}\right)dT, \tag{14}$$

where q_h is the heating rate and $T_a - T_b$ is the integration temperature range, with $T_a < T_g < T_b$.

C. Model and fitting method

The KWW function was fitted to each temperature jump dataset separately by performing regressions using Eq. (3) on the experimental refractive index and enthalpy data to obtain the parameter β. On the other hand, combined regressions were carried out for up- and down-jump experiments using the TNM model to simultaneously capture the non-exponential and non-linear nature of the aging kinetics.[3,16,20,44] To achieve this, we plotted the data using Eq. (8) and subsequently performed regressions using a numerical method to conduct the TNM fitting.

Initially, we applied Eq. (9) using the known parameters δ_0, T_0, and T. The evolution of $T_f(t)$ from T_0 to T was described by numerically integrating the reduced time using Eq. (15). For this numerical integration, we adopted the procedure detailed by Málek *et al.*,[42] where the total aging time was divided into j logarithmically spaced subintervals, with the relaxation response calculated at the end of each subinterval,

$$T_{f,j} = T + (T_0 - T)\exp\left[-\left(\sum_{j=1}^{n}\frac{\Delta t_j}{\tau_j}\right)^{\beta}\right]. \tag{15}$$

The subintervals, $\Delta t_j = t_j - t_{j-1}$, were divided into 500 logarithmic increments, and τ_j was calculated using Eq. (16),

$$\tau_j = A\exp\left(\frac{x\Delta h^*}{RT} + \frac{(1-x)\Delta h^*}{RT_{f,j-1}}\right). \tag{16}$$

Hence, the TNM model was fitted to the experimental data with β, A, and x as fitting parameters, while $\Delta h^*/R$ was fixed at 80.06 kK, obtained from the shear viscosity activation energy in the T_g region for the same LS_2 batch used in this study. Therefore, this fitting procedure assumes that the structural relaxation process has the same activation energy as that of viscous flow, as demonstrated by Moynihan *et al.*[52] through comparisons of various glass-forming systems, as well as in our recent work on the relaxation of LS_2 glass.[11] Based on the experimental data on the aging of polymers and

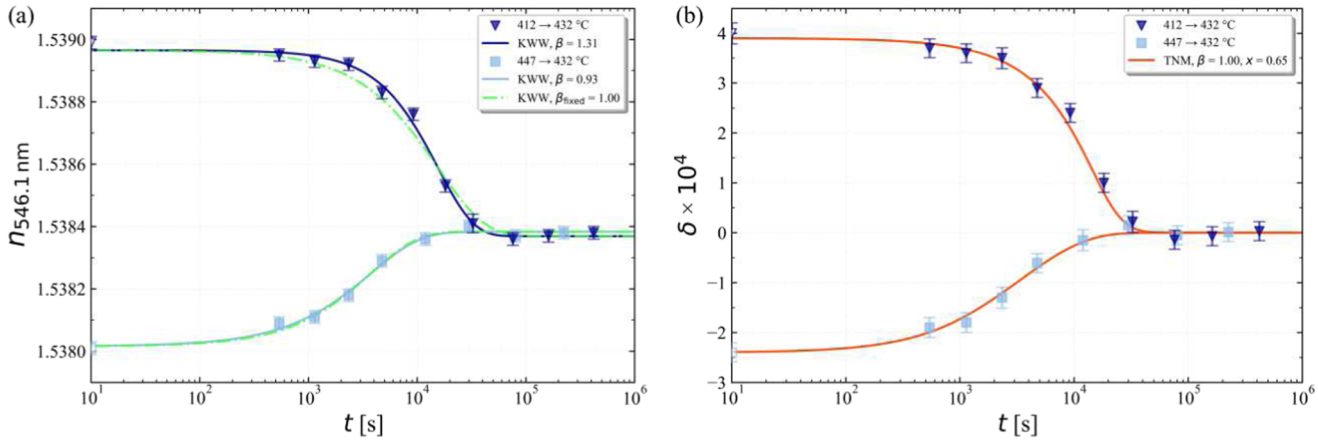

FIG. 2. Room temperature refractive index relaxation data of sample I corresponding to temperature up- and down-jumps. Filled symbols refer to the refractive index values measured over time, while open symbols indicate the values at $t = 0$ s. (a) Solid lines represent fitting curves obtained using KWW function [Eq. (3)], and dash-dotted lines correspond to fits with a fixed β value of 1.00. (b) Solid lines represent TNM model fits via Eqs. (9), (15), and (16), which describe both datasets with a single set of β and x values.

inorganic glasses reported by Hodge,[53] Boucher *et al.*[54] suggested that β and x could be correlated following an approximate linear relation: $x = \frac{\beta - 0.2}{1.05}$. However, we believe that given the spread in the experimental data, the suggested correlation is not sufficiently robust to serve as a constraint on the choice of β and x. Therefore, in the present study, we chose to vary them independently as fitting parameters.

III. RESULTS AND DISCUSSION

The room temperature refractive index of the LS_2 glass is shown in Fig. 2 as a function of aging time at 432 °C for samples pre-aged at 447 °C for 4 h and at 412 °C for 32 days. In Fig. 2(a), the refractive index variations were fitted using the KWW function, resulting in a stretching exponent of $\beta_{KWW} = 0.93$ for the temperature down-jump (447–432 °C). In contrast, the up-jump (412–432 °C) yielded

TABLE II. Summary of the KWW parameters.

	T_0 (°C)	T (°C)	p_0	p_∞	β_{KWW}	τ_K (s)
Ref. index, sample I	447	432	1.538 02	1.538 38	0.93	3711
Ref. index, sample I	412	432	1.538 96	1.538 37	1.31	15 592
Ref. index, sample II	447	422	1.537 50	1.538 15	0.56	17 822
Ref. index, sample II	422	447	1.538 14	1.537 52	1.94	3693
Enthalpy	414	444	25.2	3.1	1.22	4539
Enthalpy	414	454	24.9	0.6	1.43	1648
Enthalpy	454	444	0.8	3.3	0.87	983

TABLE III. Summary of the TNM parameters.

	T_0 (°C)	T (°C)	δ_0	Δh^* (kK)	ln (A (s))	β_{TNM}	x
Ref. index, sample I	447	432	$3 \times 10^{-5} - 1.8 \times 10^{-5}(T_0 - T)$	80.06	−104.8	1.00	0.65
Ref. index, sample I	412	432					
Ref. index, sample II	447	422	$-1.5 \times 10^{-6} - 1.71 \times 10^{-5}(T_0 - T)$	80.06	−104.2	0.85	0.50
Ref. index, sample II	422	447					
Enthalpy	414	444	$0.955 - 0.1705(T_0 - T)$	80.06	−104.3	0.90	0.66
Enthalpy	454	444					
Enthalpy	414	454	$5.988 - 0.6738(T_0 - T)$	80.06	−104.3	0.84	0.61
Enthalpy	454	444					

a compressing exponent of β_{KWW} = 1.31. Although the down-jump data can be fitted reasonably well using β_{KWW} = 1.00, this value of the non-exponentiality parameter is unable to describe the up-jump data with significant accuracy. On the other hand, in Fig. 2(b), the relaxation parameters δ were fitted using the TNM model. Both the up-jump and down-jump datasets could be fitted to the TNM model using β_{TNM} = 1.00 and x = 0.65. All parameters obtained from these fits are provided in Tables II and III, corresponding to the KWW function and the TNM model, respectively.

The DSC excess heat flow data obtained by subtracting the DSC curve of the rejuvenated glass from the aged glass are compiled in Fig. 3. The structural recovery is observed through an endothermic enthalpy overshoot at the glass transition region. In the temperature up-jump experiment, the area of the endothermic peak decreases with increasing aging times, while for the down-jump experiment, it increases with increasing aging times. Since the glass structure is frozen, its atomic mobility below glass transition is markedly reduced. During the initial aging of the material at T_0, for example, at 414 °C for 15 days, volume relaxation results in an increase in density.[12] As a result, when this sample is heated, a greater amount of energy is required for the glass transition, resulting in a larger area under the endothermic peak.[55] However, when this sample is subjected to a temperature up-jump at T, the density decreases with aging time. Therefore, as the aging time increases, the sample requires less energy for glass transition, leading to a reduction in the area under the endothermic peak.

The enthalpy recovery ΔH_R was estimated from the endothermic peaks and is represented in Fig. 4 as a function of aging time at 444 and 454 °C for samples pre-aged at 454 °C for 6.5 h and at 414 °C for 15 d. In Fig. 4(a), the KWW fit yielded a stretched exponent of β_{KWW} = 0.87 for the temperature down-jump from 454 to 444 °C. However, once again, for temperature up-jumps, it resulted in compressed exponents of β_{KWW} = 1.22 from 414 to 444 °C and β_{KWW} = 1.43 from 414 to 454 °C. Even considering the measurement uncertainties, a fixed value of β_{KWW} = 1.00 was unable to describe the up-jump data at 454 °C. Moreover, β_{KWW} increases markedly for larger temperature jumps. Figure 4(b) shows that the TNM model provides a good description of the data with somewhat similar β_{KWW} values of 0.87 and 1.22, when employing β_{TNM} = 0.90 and x = 0.66. However, as the difference between the β_{KWW} values increased for larger up- and down-jumps, the TNM model starts to exhibit a reduced capacity to describe the data. This is evident in Fig. 4(c) considering the data with β_{KWW} values of 0.87 and 1.43 for an up-jump of 40 °C, for which the TNM model was unable to describe the data using the same β_{TNM} = 0.90 and x = 0.66 (solid lines). In this particular case, the data were fitted with β_{TNM} = 0.84 and x = 0.61 (dashed lines). This is also shown in Fig. 5, where the refractive index data at $T_0 - T$ = 25 °C and $T_0 - T$ = −25 °C exhibit significantly different β_{KWW} values, both far from 1.0, as indicated by the dash-dotted green curves in Fig. 5(a). In this case, the temperature down-jump data exhibit a behavior much slower than exponential with β_{KWW} = 0.56, while the temperature up-jump data show a behavior much faster than exponential with β_{KWW} = 1.94.

Figure 5(b) shows a reasonably good fit of the TNM model to the temperature up-jump data with β_{TNM} = 1.00 and x = 0.50, but a poor fit to the down-jump data. In contrast, Fig. 5(c) shows a good fit to the down-jump data with β lower than unit, β_{TNM} = 0.70, while keeping the same x = 0.50. However, these fitting

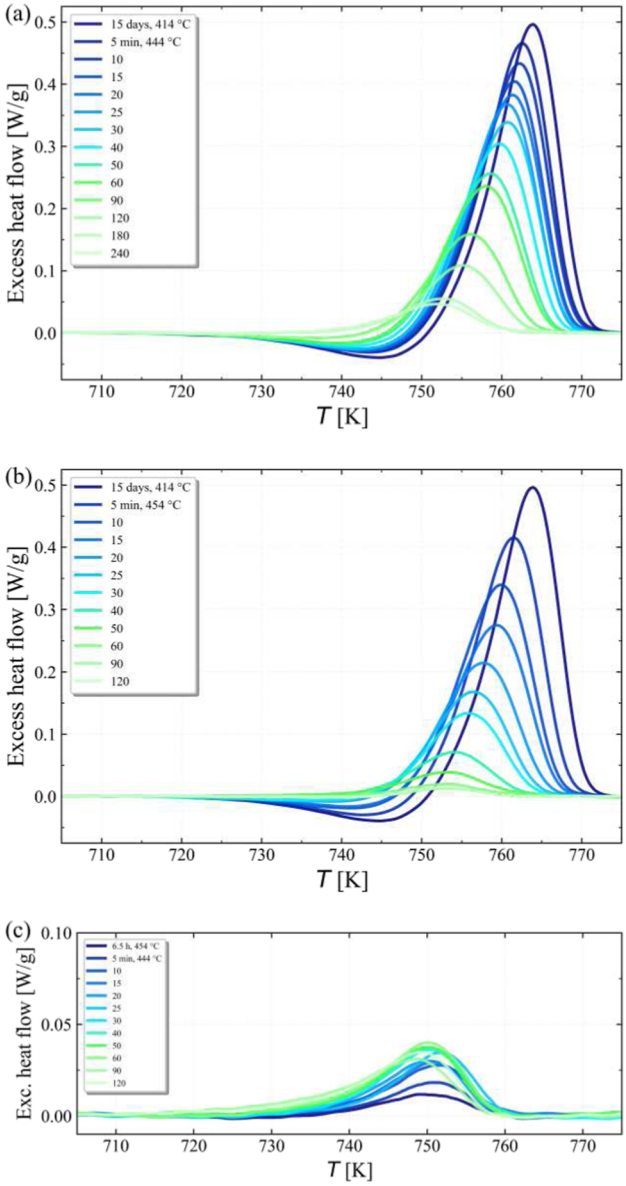

FIG. 3. Excess heat flow scans after aging from T_0 to T. (a) 414–444 °C, (b), 414–454 °C, and (c) 454–444 °C, at indicated aging times.

parameters lead to a poor description of the up-jump data. Moreover, Fig. 5(d) shows that an average value of the non-exponentiality parameter β_{TNM} = 0.85 does not provide the best fit for either dataset, but still approximately describes the data considering the measurement uncertainties.

Since our goal in this study was to test the validity of the TNM model for the relaxation kinetics of two different properties, we have made an attempt to optimize the changes in these properties to achieve the best possible experimental precision in enthalpy and refractive index measurements. As a result, we had to use different temperature jumps T_0 and T (Tables II and III), which makes

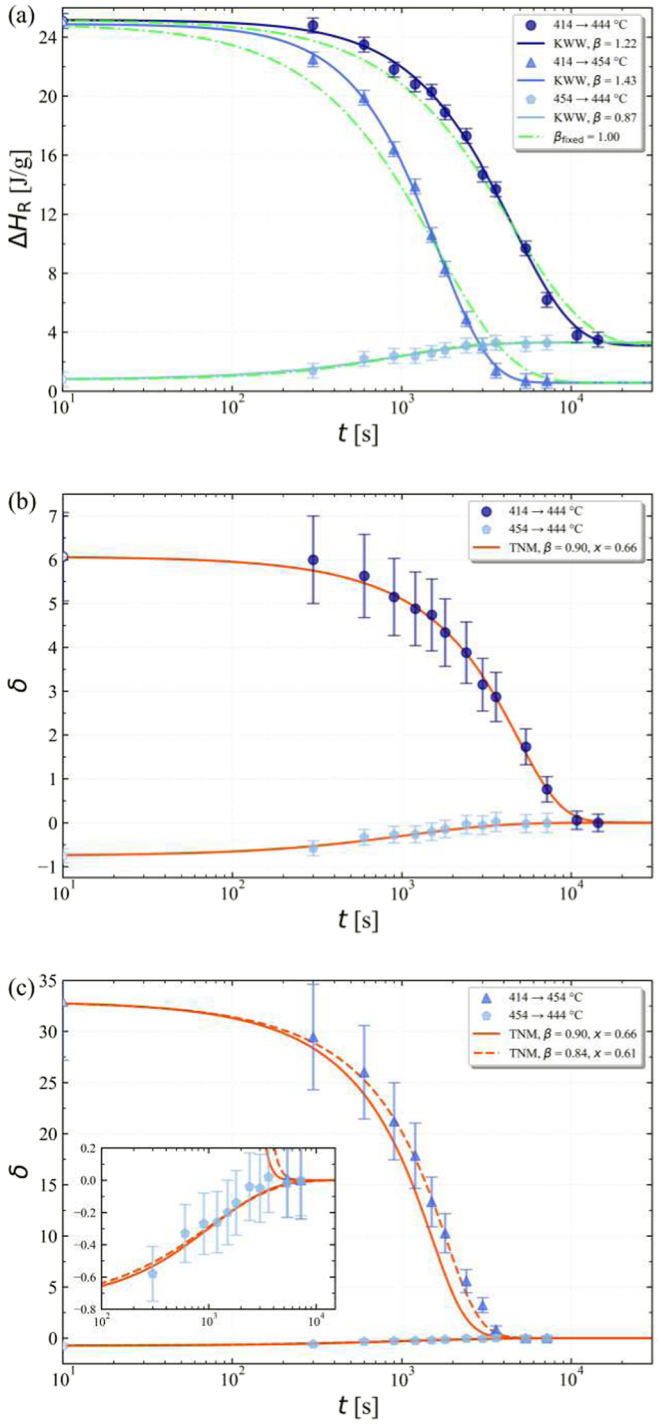

FIG. 4. Enthalpy recovery relaxation data as a function of aging time for temperature up- and down-jumps. (a) Fits obtained using the KWW function, Eq. (3). Fits obtained using the TNM model via Eqs. (9), (15), and (16) for temperature jumps from (b) 414 to 444 °C and 454 to 444 °C and (c) 414 to 454 °C and 454 to 444 °C. The inset in (c) shows a zoomed-in view of the down-jump data.

a direct comparison of the relaxation kinetics for both properties difficult. However, the fitting parameters of the TNM model β_{TNM} and x are indeed similar for the relaxation of these two properties over a similar temperature range, and good fits to the data could be obtained by keeping A fixed and similar Δh^* for all cases (Table III). Since the refractive index can be considered a reliable proxy for the sample density or volume, the observed similarity between the TNM parameters (Table III) corresponding to the relaxation of the index and enthalpy of the LS_2 glass does suggest that the physical processes responsible for enthalpy and volume relaxation are likely the same. The TNM model has proved capable of fitting both up- and down-jump datasets with $\beta \leq 1$ via introduction of the non-linearity parameter x, although it becomes progressively challenging, especially for large temperature jumps. Previous studies have also reported a similar failure of this model under these circumstances.[46–50] This result may be indicative of the fact that the TNM model, in its current form, does not include any temperature dependence of β and x, which needs to be accounted for in the case of substantial changes in T_f associated with large temperature jumps.

Physically, the compressed relaxation observed in the temperature up-jump data can be explained by considering the spatiotemporal evolution of the free volume in the structure at a given aging temperature. The structural relaxation induced rearrangement, which controls the physical aging, is a function of the thermodynamic state of the glass. When a glass is subjected to a temperature up-jump, its structure evolves from a smaller to a larger specific volume with aging time. We hypothesize that, in this case, the initial denser packing of atoms on average starts the relaxation process via nucleation events of mobile centers where the packing is less dense, i.e., the free volume is larger than average. This process results in an initially long relaxation time and slow evolution of the properties, including T_f. Eventually, these mobile centers grow in size and coalesce or percolate, leading to a rapid drop in relaxation time associated with a self-accelerated behavior characterized by an avalanche-like dynamics and compressed exponential relaxation kinetics.[24] This nucleation and growth process has been recently observed in molecular dynamics simulations of temperature up-jump experiments for the transformation of an ultrastable glass into a liquid.[56] Additionally, experimental evidence of nucleation and growth of supercooled liquid-like regions during the temperature up-jump of other glasses to $T > T_g$ has been reported in the literature.[57–59] It is worth noting here that the compressed exponential behavior is a characteristic of the Johnson–Mehl–Avrami model of transformation kinetics based on nucleation, growth, and coalescence.[60,61] In contrast, in the case of a temperature down-jump, the glass structure evolves from a larger to smaller specific volume. This reverse process does not require any nucleation event of mobile regions, as the larger initial free volume favors atom mobility, causing a rapid evolution of the properties at the beginning of the aging process. Then, as the denser regions percolate over time, it produces a self-retardation of the aging process with a stretched exponential behavior.[43] This difference in the relaxation kinetics during temperature up- and down-jumps and in the associated evolution of T_f of a glass is captured phenomenologically by the non-linearity parameter x and the non-exponentiality parameter

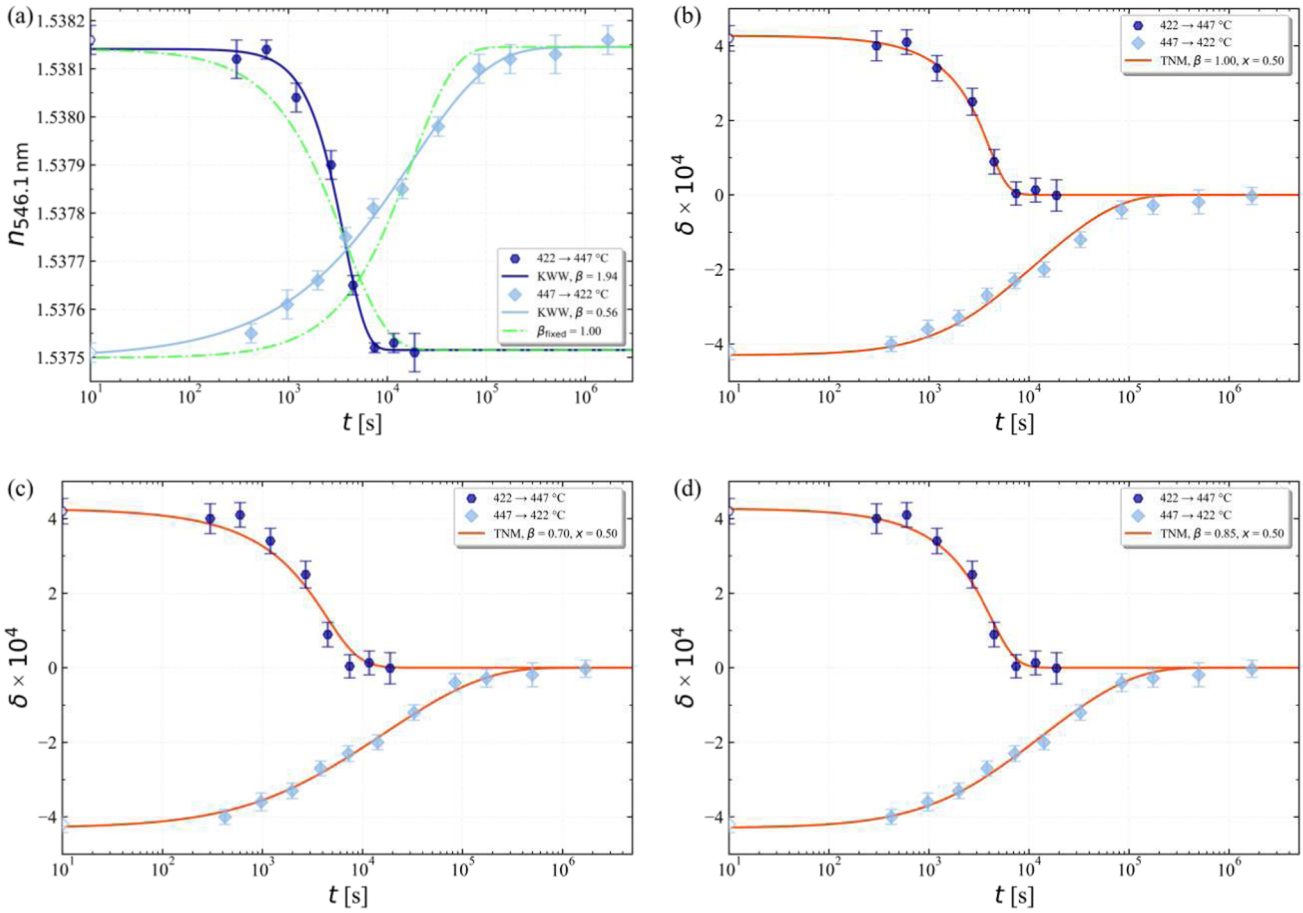

FIG. 5. Refractive index relaxation data of sample II as a function of aging time for down-jump from 447 to 422 °C and up-jump from 422 to 447 °C. (a) Best fit curves obtained using the KWW function, Eq. (3). Fitting curves using the TNM model [Eqs. (9), (15), and (16)] with $x = 0.50$ and (b) $\beta_{TNM} = 1.00$ describing the up-jump data; (c) $\beta_{TNM} = 0.70$ describing the down-jump data; (d) $\beta_{TNM} = 0.85$, which describe both datasets approximately, within the measurement uncertainties.

β of the primary or α-relaxation in the TNM model. However, it may be noted that as an alternative explanation for the compressed relaxation observed in the temperature up-jumps, as well as to account for the failure of the TNM model, the possible involvement of mechanisms distinct from those corresponding to the α-relaxation has also been discussed in the literature.[49,50,62]

IV. CONCLUSIONS

We tested the validity of the TNM model in describing the relaxation kinetics associated with isothermal physical aging of glasses for large temperature jumps. An analysis of the structural relaxation process using the KWW expression revealed distinct kinetic behaviors for temperature up- and down-jumps, associated with the non-linearity of glassy relaxation. Specifically, the down-jump data exhibit a stretched exponential behavior ($\beta < 1$), whereas the up-jump data display a compressed exponential behavior ($\beta > 1$). The non-exponentiality of the kinetics increases with the increase of the magnitude of the temperature jump. However, both up- and down-jump datasets can be fitted simultaneously using the TNM model with a single set of A, Δh^*, $\beta \leq 1$, and $x < 1$, especially when the temperature jump is relatively small, resulting in a comprehensive mathematical description of the relaxation process. However, as the magnitude of the temperature jump increases, the TNM model fails to accurately fit both datasets exhibiting compressed and stretched behaviors. This failure likely arises from the TNM model's treatment of β and x as temperature-independent variables in a phenomenological manner. This approximation is probably inadequate for large temperature jumps, when T_f of the glass varies significantly during the relaxation process.

ACKNOWLEDGMENTS

We are grateful for the support from the São Paulo Research Foundation (FAPESP), Project Grant No. 2013/07793-6 (CEPID), student Grant No. 2021/03374-5 (R.F.L.), and the Brazil–United States cooperation under Grant No. 2022/07679-8. S.S. acknowledges the support from the Blacutt–Underwood endowed

professorship grant at UC Davis. This study was financed, in part, by the Coordenação de Aperfeiçoamento de Pessoal de Nível Superior—Brasil (CAPES)—Finance Code 001.

AUTHOR DECLARATIONS

Conflict of Interest

The authors have no conflicts to disclose.

Author Contributions

Ricardo F. Lancelotti: Conceptualization (equal); Data curation (lead); Formal analysis (equal); Investigation (lead); Methodology (equal); Writing – original draft (lead). **Edgar D. Zanotto**: Conceptualization (equal); Formal analysis (equal); Funding acquisition (lead); Resources (equal); Supervision (equal); Validation (equal); Writing – review & editing (equal). **Sabyasachi Sen**: Conceptualization (equal); Formal analysis (equal); Resources (equal); Supervision (equal); Validation (equal); Writing – review & editing (equal).

DATA AVAILABILITY

The data that support the findings of this study are available within the article.

REFERENCES

[1]A. Q. Tool, "Relaxation of stresses in annealing glass," J. Res. Natl. Bur. Stand. **34**(2), 199–211 (1945).
[2]K. A. Kirchner, D. R. Cassar, E. D. Zanotto, M. Ono, S. H. Kim, K. Doss, M. L. Bødker, M. M. Smedskjaer, S. Kohara, L. Tang, M. Bauchy, C. J. Wilkinson, Y. Yang, R. S. Welch, M. Mancini, and J. C. Mauro, "Beyond the average: Spatial and temporal fluctuations in oxide glass-forming systems," Chem. Rev. **123**, 1774–1840 (2023).
[3]O. S. Narayanaswamy, "A model of structural relaxation in glass," J. Am. Ceram. Soc. **54**(10), 491–498 (1971).
[4]E. D. Zanotto and J. C. Mauro, "The glassy state of matter: Its definition and ultimate fate," J. Non-Cryst. Solids **471**, 490–495 (2017).
[5]G. W. Scherer, "Volume relaxation far from equilibrium," J. Am. Ceram. Soc. **69**(5), 374–381 (1986).
[6]M. Micoulaut, "Relaxation and physical aging in network glasses: A review," Rep. Prog. Phys. **79**(6), 066504 (2016).
[7]C. J. Wilkinson, K. Doss, O. Gulbiten, D. C. Allan, and J. C. Mauro, "Fragility and temperature dependence of stretched exponential relaxation in glass-forming systems," J. Am. Ceram. Soc. **104**(9), 4559–4567 (2021).
[8]A. Winter, "Transformation region of glass," J. Am. Ceram. Soc. **26**(6), 189–200 (1943).
[9]S. Spinner and A. Napolitano, "Further studies in the annealing of a borosilicate glass," J. Res. Natl. Bur. Stand., Sect. A **70A**, 147–152 (1966).
[10]R. F. Lancelotti, A. C. M. Rodrigues, and E. D. Zanotto, "Structural relaxation dynamics of a silicate glass probed by refractive index and ionic conductivity," J. Am. Ceram. Soc. **106**, 5814–5821 (2023).
[11]R. F. Lancelotti, T. R. Cunha, M. A. C. Kurtovic, P. S. Pizani, S. Sen, and E. D. Zanotto, "Physical aging of lithium disilicate glass," J. Non-Cryst. Solids **622**, 122661 (2023).
[12]H. N. Ritland, "Density phenomena in the transformation range of a borosilicate crown glass," J. Am. Ceram. Soc. **37**(8), 370–377 (1954).
[13]M. Hara and S. Suetoshi, "Density change of glass in transformation range," Report No. 2, Report of the Research Laboratory, Asahi Glass Co., 1955, Vol. **5**, pp. 126–135.
[14]B. Yuan, H. Chen, and S. Sen, "Aging-induced structural evolution of a $GeSe_2$ glass network: The role of homopolar bonds," J. Phys. Chem. B **126**(4), 946–952 (2022).
[15]S. Jurca, H. Chen, and S. Sen, "Structural, shear and volume relaxation in a commercial float glass during aging," J. Non-Cryst. Solids **589**, 121650 (2022).
[16]I. M. Hodge and A. R. Berens, "Effects of annealing and prior history on enthalpy relaxation in glassy polymers. 2. Mathematical modeling," Macromolecules **15**(3), 762–770 (1982).
[17]S. J. Schmidt and A. M. Lammert, "Physical aging of maltose glasses," J. Food Sci. **61**(5), 870–875 (1996).
[18]A. Czerniecka-Kubicka, I. Zarzyka, and M. Pyda, "Long-term physical aging tracked by advanced thermal analysis of poly(*N*-isopropylacrylamide): A smart polymer for drug delivery system," Molecules **25**(17), 3810 (2020).
[19]E. A. King, S. Sen, W. Takeda, C. Boussard-Pledel, B. Bureau, J.-P. Guin, and P. Lucas, "Extended aging of Ge–Se glasses below the glass transition temperature," J. Chem. Phys. **154**(16), 164502 (2021).
[20]C. T. Moynihan, P. B. Macedo, C. J. Montrose, C. J. Montrose, P. K. Gupta, M. A. DeBolt, J. F. Dill, B. E. Dom, P. W. Drake, A. J. Easteal *et al.*, "Structural relaxation in vitreous materials," Ann. N. Y. Acad. Sci. **279**(1), 15–35 (1976).
[21]R. Kohlrausch, "Theorie des elektrischen Rückstandes in der Leidener Flasche," Ann. Phys. **167**(2), 179–214 (1854).
[22]G. Williams and D. C. Watts, "Non-symmetrical dielectric relaxation behaviour arising from a simple empirical decay function," Trans. Faraday Soc. **66**, 80–85 (1970).
[23]M. Potuzak, R. C. Welch, and J. C. Mauro, "Topological origin of stretched exponential relaxation in glass," J. Chem. Phys. **135**(21), 214502 (2011).
[24]K. Trachenko and A. Zaccone, "Slow stretched-exponential and fast compressed-exponential relaxation from local event dynamics," J. Phys.: Condens. Matter **33**(31), 315101 (2021).
[25]P. Debye, *Polar Molecules* (The Chemical Catalog Company, Inc., New York, 1929), Vol. 89.
[26]J. C. Phillips, "Kohlrausch explained: The solution to a problem that is 150 years old," J. Stat. Phys. **77**(3–4), 945–947 (1994).
[27]J. C. Phillips, "Stretched exponential relaxation in molecular and electronic glasses," Rep. Prog. Phys. **59**(9), 1133 (1996).
[28]K. L. Ngai, *Relaxation and Diffusion in Complex Systems* (Springer Science+Business Media, New York, 2011).
[29]R. F. Lancelotti, D. R. Cassar, M. Nalin, O. Peitl, and E. D. Zanotto, "Is the structural relaxation of glasses controlled by equilibrium shear viscosity?," J. Am. Ceram. Soc. **104**(5), 2066–2076 (2021).
[30]R. Richert, "Heterogeneous dynamics in liquids: Fluctuations in space and time," J. Phys.: Condens. Matter **14**(23), R703 (2002).
[31]G. N. Greaves and S. Sen, "Inorganic glasses, glass-forming liquids and amorphizing solids," Adv. Phys. **56**(1), 1–166 (2007).
[32]A. Cavagna, "Supercooled liquids for pedestrians," Phys. Rep. **476**(4–6), 51–124 (2009).
[33]P. Falus, M. A. Borthwick, S. Narayanan, A. R. Sandy, and S. G. J. Mochrie, "Crossover from stretched to compressed exponential relaxations in a polymer-based sponge phase," Phys. Rev. Lett. **97**(6), 066102 (2006).
[34]B. Ruta, Y. Chushkin, G. Monaco, L. Cipelletti, E. Pineda, P. Bruna, V. M. Giordano, and M. Gonzalez-Silveira, "Atomic-scale relaxation dynamics and aging in a metallic glass probed by x-ray photon correlation spectroscopy," Phys. Rev. Lett. **109**(16), 165701 (2012).
[35]E. W. Hansen, X. Gong, and Q. Chen, "Compressed exponential response function arising from a continuous distribution of Gaussian decays – distribution characteristics," Macromol. Chem. Phys. **214**(7), 844–852 (2013).
[36]Z. W. Wu, W. Kob, W.-H. Wang, and L. Xu, "Stretched and compressed exponentials in the relaxation dynamics of a metallic glass-forming melt," Nat. Commun. **9**(1), 5334 (2018).
[37]M. Guerette, M. R. Ackerson, J. Thomas, E. B. Watson, and L. Huang, "Thermally induced amorphous to amorphous transition in hot-compressed silica glass," J. Chem. Phys. **148**(19), 194501 (2018).
[38]Q. Li, X. Peng, and G. B. McKenna, "Physical aging and compressed exponential behaviors in a model soft colloidal system," Soft Matter **15**(11), 2336–2347 (2019).

[39]D. Diaz Vela and D. S. Simmons, "The microscopic origins of stretched exponential relaxation in two model glass-forming liquids as probed by simulations in the isoconfigurational ensemble," J. Chem. Phys. **153**(23), 234503 (2020).
[40]K. Mithra and S. S. Jena, "Surfactant head group and concentration influence on structure and dynamics of gellan gum hydrogels: Crossover from stretched to compressed exponential," J. Polym. Sci. **59**(17), 1972–1985 (2021).
[41]T. D. Jaeger and D. S. Simmons, "Temperature dependence of aging dynamics in highly non-equilibrium model polymer glasses," J. Chem. Phys. **156**(11), 114504 (2022).
[42]J. Málek, R. Svoboda, P. Pustková, and P. Čičmanec, "Volume and enthalpy relaxation of a-Se in the glass transition region," J. Non-Cryst. Solids **355**, 264–272 (2009).
[43]D. Cangialosi, V. M. Boucher, A. Alegría, and J. Colmenero, "Physical aging in polymers and polymer nanocomposites: Recent results and open questions," Soft Matter **9**(36), 8619–8630 (2013).
[44]A. Q. Tool, "Relation between inelastic deformability and thermal expansion of glass in its annealing range," J. Am. Ceram. Soc. **29**(9), 240–253 (1946).
[45]I. M. Hodge, "Physical aging in polymer glasses," Science **267**(5206), 1945–1947 (1995).
[46]G. B. McKenna and C. A. Angell, "The phenomenology and models of the kinetics of volume and enthalpy in the glass transition range," J. Non-Cryst. Solids **131–133**, 528–536 (1991).
[47]J. C. Mauro, D. C. Allan, and M. Potuzak, "Nonequilibrium viscosity of glass," Phys. Rev. B **80**(9), 094204 (2009).
[48]R. Svoboda and J. Málek, "Description of enthalpy relaxation dynamics in terms of TNM model," J. Non-Cryst. Solids **378**, 186–195 (2013).
[49]V. Di Lisio, V.-M. Stavropoulou, and D. Cangialosi, "Physical aging in molecular glasses beyond the α relaxation," J. Chem. Phys. **159**(6), 064505 (2023).
[50]A. Toda, "Isothermal enthalpy relaxation of amorphous polystyrene studied using temperature-modulated fast scanning calorimetry," Thermochim. Acta **721**, 179433 (2023).
[51]D. R. Cassar, A. H. Serra, O. Peitl, and E. D. Zanotto, "Critical assessment of the alleged failure of the classical nucleation theory at low temperatures," J. Non-Cryst. Solids **547**, 120297 (2020).
[52]C. T. Moynihan, S.-K. Lee, M. Tatsumisago, and T. Minami, "Estimation of activation energies for structural relaxation and viscous flow from DTA and DSC experiments," Thermochim. Acta **280–281**, 153–162 (1996).
[53]I. M. Hodge, "Adam-Gibbs formulation of enthalpy relaxation near the glass transition," J. Res. Natl. Inst. Stand. Technol. **102**(2), 195 (1997).
[54]V. M. Boucher, D. Cangialosi, A. Alegría, and J. Colmenero, "Enthalpy recovery of glassy polymers: Dramatic deviations from the extrapolated liquidlike behavior," Macromolecules **44**(20), 8333–8342 (2011).
[55]P. Pan, B. Zhu, and Y. Inoue, "Enthalpy relaxation and embrittlement of poly(L-lactide) during physical aging," Macromolecules **40**(26), 9664–9671 (2007).
[56]C. Herrero, C. Scalliet, M. D. Ediger, and L. Berthier, "Two-step devitrification of ultrastable glasses," Proc. Natl. Acad. Sci. U. S. A. **120**(16), e2220824120 (2023).
[57]K. L. Kearns, M. D. Ediger, H. Huth, and C. Schick, "One micrometer length scale controls kinetic stability of low-energy glasses," J. Phys. Chem. Lett. **1**(1), 388–392 (2010).
[58]A. Vila-Costa, J. Ràfols-Ribé, M. González-Silveira, A. F. Lopeandia, L. Abad-Muñoz, and J. Rodríguez-Viejo, "Nucleation and growth of the supercooled liquid phase control glass transition in bulk ultrastable glasses," Phys. Rev. Lett. **124**(7), 076002 (2020).
[59]A. Vila-Costa, M. Gonzalez-Silveira, C. Rodríguez-Tinoco, M. Rodríguez-López, and J. Rodriguez-Viejo, "Emergence of equilibrated liquid regions within the glass," Nat. Phys. **19**(1), 114–119 (2023).
[60]J. William and R. Mehl, "Reaction kinetics in processes of nucleation and growth," Trans. Am. Inst. Min. Metall. Eng. **135**, 416–442 (1939).
[61]M. Avrami, "Kinetics of phase change. I General theory," J. Chem. Phys. **7**(12), 1103–1112 (1939).
[62]J. M. O'Reilly, "Review of structure and mobility in amorphous polymers," Crit. Rev. Solid State Mater. Sci. **13**(3), 259–277 (1987).